

Analysis of Velocity Profiles in Rectangular Straight Open Channel Flow

Abinash Sahoo^{1*}, Sandeep Samantaray¹ and Rosysmita Bikram Singh²

¹Department of Civil Engineering, National Institute of Technology Silchar, Assam 788010, India

²Department of Civil Engineering, Veer Surendra Sai University of Technology Burla, Odisha 768018, India

ABSTRACT

This study aims at analysing the velocity profiles in a straight rectangular channel having a constant width and depth throughout the channel length. Experiment was conducted for five altered depths using the straight rectangular flume in hydraulic flow laboratory available at VSS University of Technology, Odisha, India. Furthermore, the distributions of stream wise velocity at the different flow depth were computed numerically using hydraulic software ANSYS FLUENT 18.1. The results of numerical simulation showed sensibly good agreement with experimental data, which was $\pm 10\%$ for both across and along the channel of rectangular flume. The Reynolds number in this study lay between 10,853 to 79,000. In case of channel flow, the velocity varied both in longitudinal and transverse direction. The isovel lines joining points of equal velocity normally curved upward due to the effect of turbulence. Peak velocity was found below the free surface of water. The law of logarithmic and power law was applied to study velocity distribution in terms of turbulent flow condition. The model could be validated by considering the various parameters of flow measurement such as the resultant velocity and the velocity at both horizontal and vertical direction. The inclusive idea of this study was to comprehend flow characteristic over a plane bed through experimental and numerical simulation methods.

Keywords: ANSYS, logarithmic law, power law, rectangular flume, velocity distribution, velocity profile

ARTICLE INFO

Article history:

Received: 13 January 2019

Accepted: 19 July 2019

Published: 13 January 2020

E-mail addresses:

bablushahoo1992@gmail.com (Abinash Sahoo)

samantaraysandeep963@gmail.com (Sandeep Samantaray)

puja003@gmail.com (Rosysmita Bikram Singh)

* Corresponding author

INTRODUCTION

The distribution of longitudinal component of velocity in a given cross-section is a significant parameter in the study of an open channel flow to find out various properties of flow. Diverse and complex behaviour of fluid flow which occurs at a particular period generates intricate structures that

have to be modelled or solved partially based on time and length scale. Hence a study of a consistent mathematical model of velocity distribution is frequently needed. Study of velocity distribution pattern indicates there is a rise in velocity consistently with vertical distance from bed of the channel. At lower depths of flow, magnitude of velocity is least at the bed because of no slip condition while velocity is found to be highest at some point below the free surface. When there is an increase in depth, the sequences of greater velocity occurs at free surface of the wall.

Bonakdari et al. (2014) developed a 3D Computational Fluid Dynamics (CFD) model using ANSYS software to examine flow patterns and the $k-\epsilon$ turbulence closure model was applied to resolve turbulence equations. Wake function is unable to detect the action of secondary currents and thus is not applicable to 3D flows, as it helps in predicting an increasing velocity with distance from the bed. Coles (1956) found that $k-\epsilon$ model took into account two equations for isotropic turbulence. Hence, model is inadequate to speculate the secondary currents and velocity-dip-phenomenon related to it. Nezu and Rodi (1986) and Cardoso et al. (1989) applied the classical log law to determine velocity profile for vertical flow in an open channel at a section $\xi < 0.2$ $\{\xi = y/h$, is ratio between distance from bed(y) to flow depth (h)}. Castro-Orgaz, and Dey (2011) proposed theory of power-law for velocity profile for flow under turbulent boundary layer. Naik et al. (2018) used ANSYS-Fluent software to simulate the model in two phases numerically in a converging compound channel. Welahettige et al. (2017) used ANSYS Fluent R16.2 for CFD simulations and outcomes were validated with experimental results done in an open Venturichannel. Naot et al. (1993) applied Log-wake and power law to narrate flows in two-dimensional open-channel. Kang and Choi (2006) gave additional advanced RANS equations based on anisotropic turbulence models and should be used for prediction of velocity-dip-phenomena. Sarma et al. (2000) described velocity distribution taking into consideration velocity dip for flow in open channel. They used binary version of velocity distribution, where inner section follows logarithmic law and outer section follows parabolic law. Afzal et al. (2007) used Velocity profile power law to cover the influence of friction in fully developing zone for turbulent pipe and open channel flows. Wilkerson and McGahan (2005) expanded two models which help in predicting depth-averaged velocity distributions. Guo and Julien (2006) derived modified-log-wake law to predict velocity-dip-phenomenon for flow in open channel. Absi (2011) modified this law and proposed another law for velocity profile called the full dip-modified-log-wake law and law was semi analytical.

The purpose of this study is to compute magnitude of velocity at various points longitudinally and laterally of the rectangular flume, which assists to draw the velocity flow profiles that help in studying the velocity distribution and its characteristics. The resulting velocity profiles are validated with the universal laws. The results found from this computational approach are hence contrasted with the experimental data for better

efficiency. The computational way is considerably being used globally due to competency and flow complexity, which helps in resolving and modelling instinctively in accordance to what the model requires.

METHODS

Theoretical Consideration

Study from literature suggested that in an open channel the magnitude of velocity is maximum at some point below top surface of water. For narrow channels where the aspect ratio $Ar < 5$, the occurrence of maximum velocity is below free surface of water. By assuming “shear stress is constant”, P-vK (Prandtl-von Karman) law is considered as general form of velocity distribution, applied near channel bed. The von Karman constant is modified and it can be applied in outer region of flow. P-vK law overlaps with log law at about 20% of flow depth and can be used for full flow depth. Log law is strictly applicable to the region below 20% of flow depth that may be attributed to the law of the wall (log-law) which is often applied to the entire depth. Log law is effective for inner region near the bed, but it will be deviated from the laboratory data on the outer layer:

$$\frac{u}{u_*} = \frac{1}{k} \left[\text{Ln} \left(\frac{y}{y_0} \right) \right] \quad (1)$$

Where, u = mean velocity in main flow direction

u_* = shear velocity

y = upright distance from bed

y_0 = distance where velocity is hypothetically zero

k denotes the von-Karman constant. For outer region of flow i.e. $\xi > 0.2$, there is a variance of log law from experimental data. So, for two-dimensional flows, this variance was adjusted by summing Coles wake function as

$$\frac{u}{u_*} = \frac{1}{k} \left[\ln \left(\frac{y}{y_0} \right) + 2\Pi \sin^2 \left(\frac{\pi y}{2h} \right) \right] \quad (2)$$

Where h = flow depth

Π = Coles' wake strength. The expression is called the log wake law, notation Π express the Coles parameter, denoting the wake function strength. General form of parabolic law given by:

$$\frac{u - u_{\max}}{u_*} = 6.3 \left(1 - \frac{\eta}{\eta_{\text{dip}}} \right)^2 \quad (3)$$

Where η = dimensionless distance from bed

η_{dip} = dimensionless distance of maximum velocity.

On basis of the intersection point, the parabolic law is valid to the free surface which ranges from 0.2 to 0.3 for flows in sediment-laden. Later, Coles proposed the limitations of the law and validity region for parabolic law. For a narrow channel where the aspect ratio $Ar < 5$, peak velocity occurs below free surface of water, resulting in phenomenon of velocity-dip-, which involves a variance from log-wake law. Using the laws proposed by Coles, velocity profile was validated in this present study.

Experimental Setup

Experiments were conducted utilizing the flume present in the Hydraulics Lab of VSSUT, Burla as shown in Figure 1. The experiments were performed in a straight simple rectangular flume described below in Figure 2 made of iron whose length is 2.5 m, width 0.3 m, and 0.3 m deep. The water supply was from a storage sump which was lifted by a number of parallel pumps to an overhead tank. From the overhead tank water was carried to the flume and discharge was controlled through a valve. The head gate was lifted fully to allow the water to enter the flume. Baffle walls were provided in series before the head gate so as to decrease the turbulence effect of the incoming water. The Point gauge was first checked for its smooth moving over the flume and its least count was noted. The tail-gate was responsible to maintain the uniformity of flow which was accumulated in a metal tank,

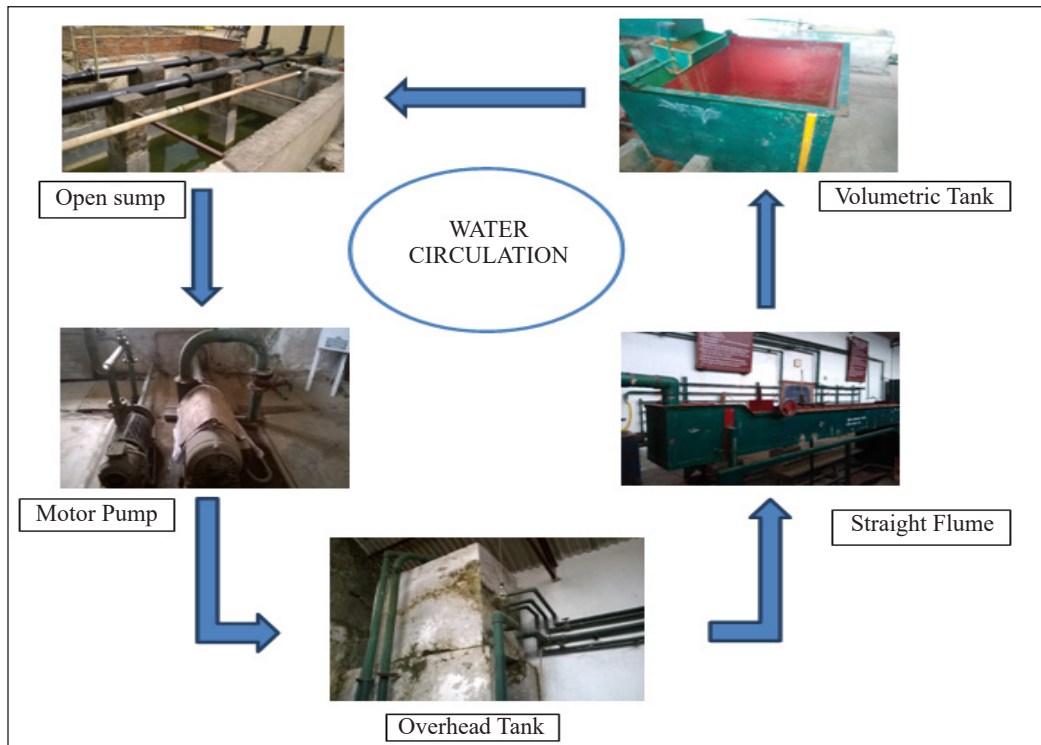


Figure 1. Experimental setup in the Lab

where the volumetric measurement could be taken. Further it can be redirected to the sump and from sump to overhead tank, with a help of a pump installed in the laboratory, thus setting a complete re-circulating water supply system to the flume. To attain a steady and uniform flow conditions every single experimental run of the flume was done by keeping the water surface gradient parallel to the bed slope.

The flow velocity in the experiment were measured at 9 mid-verticals ($x = 0.25, 0.5, 0.75, 1.0, 1.25, 1.5, 1.75, 2.0, 2.25$ m) alongside the flow developing region and 6 mid-horizontals ($y = 0.03, 0.06, 0.09, 0.12, 0.15$ and 0.18 m) across the flow developing zone across half width of the flow section revealed in Figure 2. This was for a single water flow depth. In this way, the same procedure was repeated for multiple flow depths starting from bed of the channel ($0.06, 0.1, 0.14, 0.18, 0.22$ m).

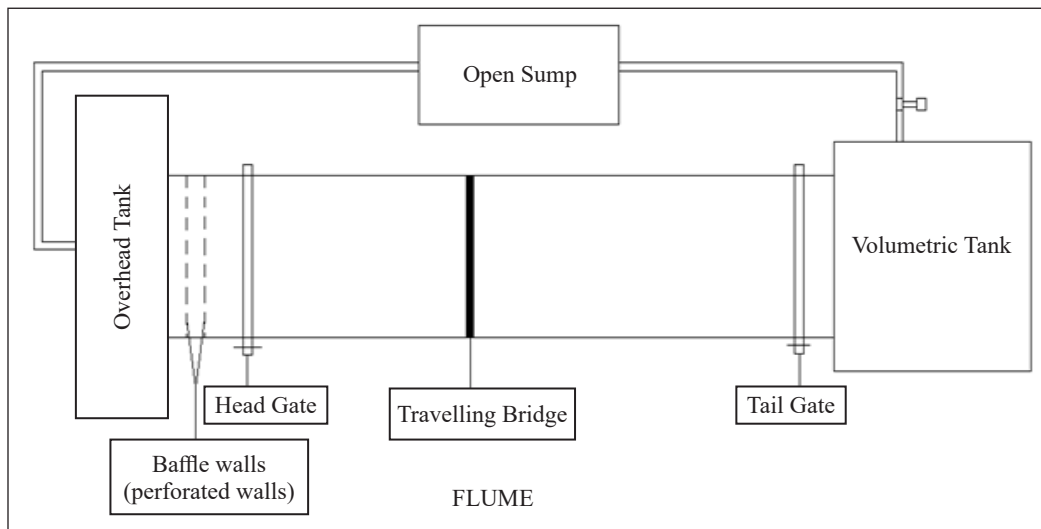


Figure 2. Plan view of the experimental flume

Table 1
Details of the experimental conditions

Test No.	Flow Discharge, Q (cm ³ /s)	Height, h (m)	Aspect Ratio, b/h	Froude number (F _r)	Reynolds number (R _c)
1	19.55	0.06	5	0.29	10,853
2	27.2	0.1	3	0.323	21,573
3	38.25	0.14	2.14	0.384	36,404
4	51	0.18	1.66	0.451	54,606
5	67.15	0.22	1.36	0.537	79,000

Table 1 indicates the different heights from channel bed where the velocity measurements have been conducted with different aspect ratio. F_r -Froude number = V/\sqrt{gh} , where V-average velocity, R_c -Reynolds number = VR/ν where R-hydraulic radius.

Depth of flow in rectangular channel was measured through piezometer which was static on the traveling bridge and manually functioned. We can note the height of water entering into the tank and with the help of a stopwatch we can calculate the time. Dividing height by time we obtained the velocity and then multiplying it with the base area of the tank we obtained the average discharge. The velocity of the flow was measured at various points using a Pitot tube connected to a manometer. While noting velocity readings using Pitot tube, Pitot was positioned facing towards the flow direction. After this setup it was again turned across flow direction. Along the longitudinal section of rectangular flume pitot was moved at 0.25 m intervals in horizontal direction and 0.2h, 0.4h, 0.6h, 0.8h (h-flow depth) just below free surface of the respective flow depth in vertical direction. Similarly, along lateral section of the flume pitot was moved at 0.03m intervals in horizontal direction and 0.2h, 0.4h, 0.6h, 0.8h below free surface in vertical direction as depicted in Figure 3. As the cross-section of channel was square in shape, velocity was measured from near side wall till mid interval of the channel because the magnitude of velocity remained same on the other half of the interval. The Pitot tube was fixed to primary scale which had least count of 0.1 mm with the Vernier scale. To the right limb of the Pitot the pipe was attached to the right limb of the manometer and the left limb of the pitot to the left limb. The velocity hence was calculated by formula:

$$V = \sqrt{2g\Delta H} \quad (4)$$

where g -force of gravity, ΔH -water elevation difference in the manometer.

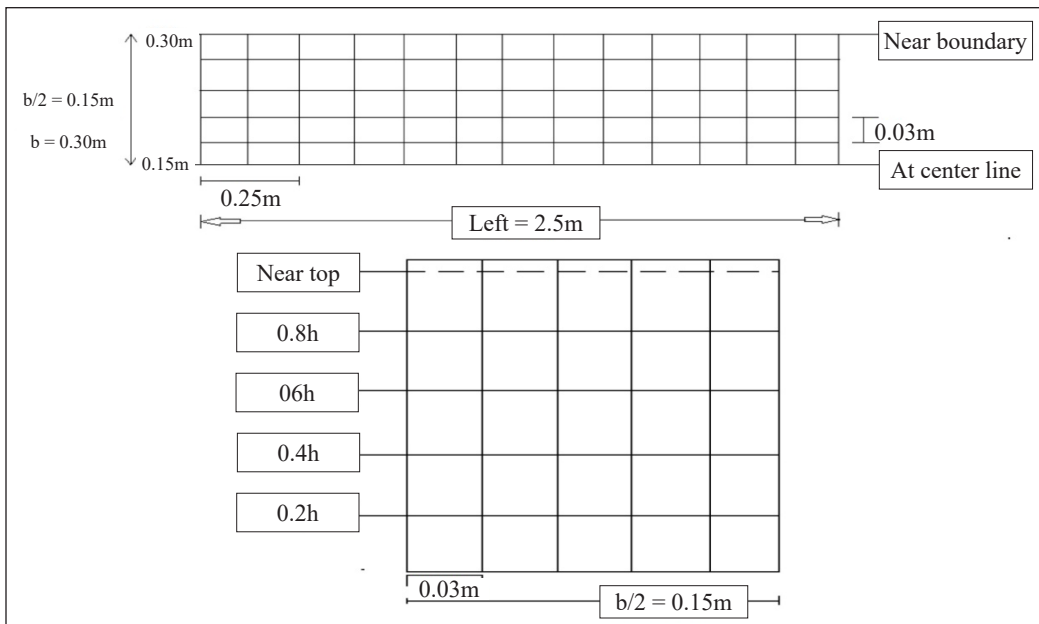


Figure 3. Detail plan (a) and cross-section (b) of experimental grid where velocity measured

NUMERICAL MODEL SETUP

A flow through the open channel is dependent on the various features such as bed properties, shear resistance and friction. k- ϵ model is highly adopted model in CFD to simulate characteristics of flow in turbulent flow condition. Larocque et al. (2013) proposed k- ϵ model which emphasised on mechanisms that impacted on turbulent kinetic energy. This kind of generality is lacking in the mixing length model. Assumptions made for the model is 'the average rate of distortions is alike in all directions'. It is a semi-empirical model which depends on model transport equations for turbulent-kinetic energy ' k ' and dissipation rate ' ϵ '. Simulation of flow model can be solved in an efficient manner with the help of ANSYS (Fluent). The cross-section of the rectangular flume used for the experimental purpose is drawn with the help of ANSYS software and is divided into different sections with plates placed both in horizontal and vertical directions as revealed in Figure 4 for numerical analysis. The fluid flow equation is governed by momentum equation and continuity equation. This method is fit for structured as well as unstructured mesh.

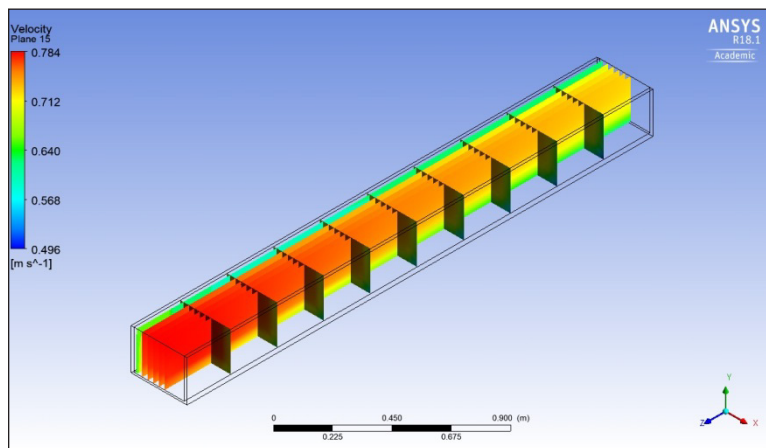


Figure 4. Cross-sectional plates along and across the flow direction

Boundary Conditions

Near wall and channel bed the components of velocity become zero due to effect of no slip condition. For the free surface, the boundary conditions are symmetric that is *no scalar flux takes place across the boundary*. The truncation error that arises by stepwise approximation can be controlled by providing a very fine Cartesian mesh. Nodes are required for the area near the wall and the wake regions. For this case study under consideration the flow domain was discretized by the use of structured grid and body-fitted coordinates. The meshing details of flume are indicated in Figure 5. Least size of the grid after meshing is 0.2527 mm and maximum size of the grid is found be 50.55 mm. The maximum face size of the flume is kept 25.27 mm. Grid size may vary depending on different model setup.

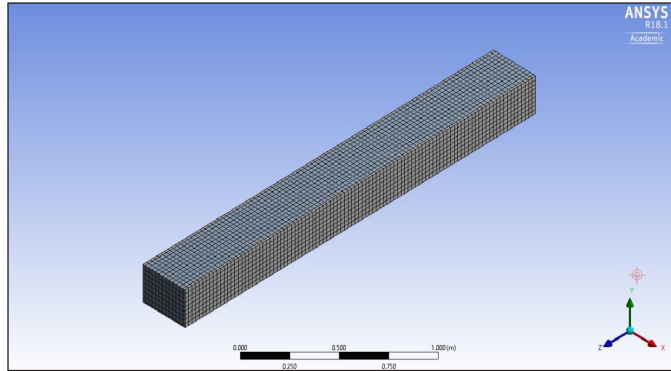


Figure 5. Meshing of the Flume in 3-D ANSYS

Application of Numerical Analysis

In present study, the coupling among velocity field and pressure field is complemented by PISO technique, which is pressure implicit splitting operator available in Fluent as proposed by (Issa, 1986). Figure 6, 7 and 8 show the velocity distribution in stream-wise, vertical, lateral direction and the resultant velocity distribution at 0.25, 1.25 and 2.25 m from the head gate for no load conditions as simulated in ANSYS. In the present work, it is observed that the results obtained from ANSYS were matching well with the experimental data and magnitude of maximum velocity and velocity distribution were virtually equal to the results derived experimentally.

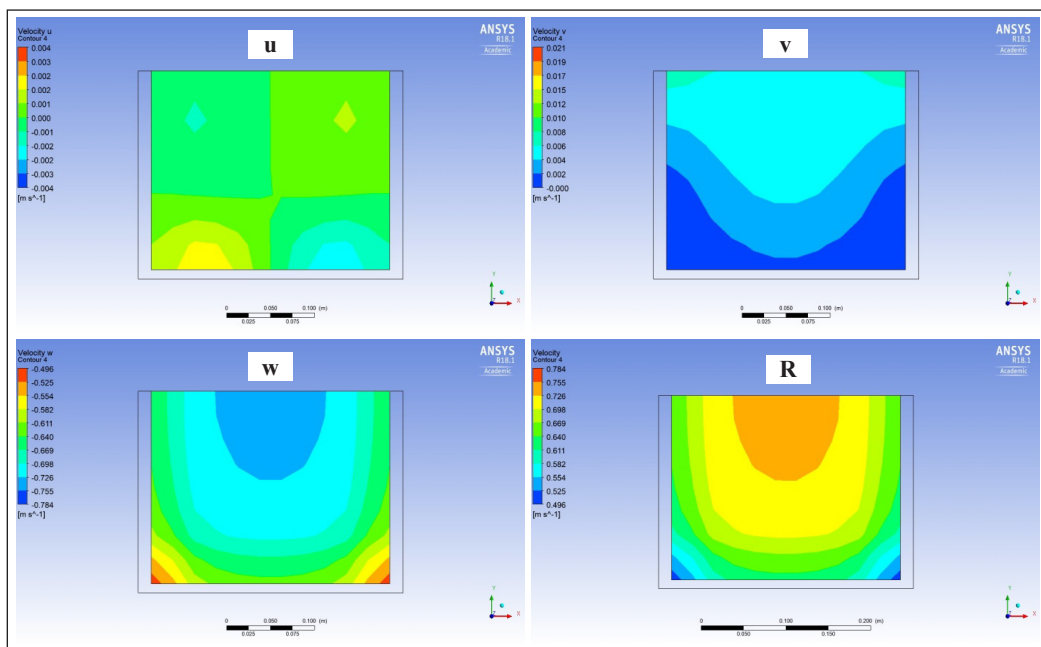


Figure 6. Contours for stream wise velocity (u), vertical velocity (v), lateral velocity (w), resultant velocity (R) at 0.25m from head

Analysis of Velocity Profiles in Rectangular Straight Open Channel Flow

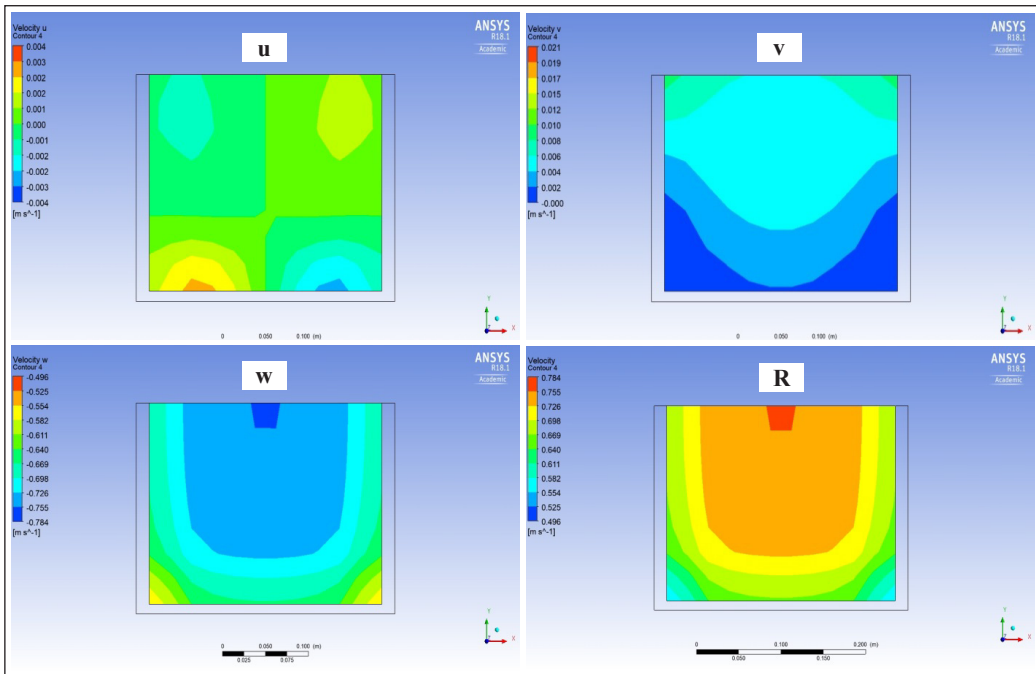


Figure 7. Contours for stream wise (u), velocity vertical velocity (v), lateral velocity (w), resultant velocity (R) at 1.5m from head

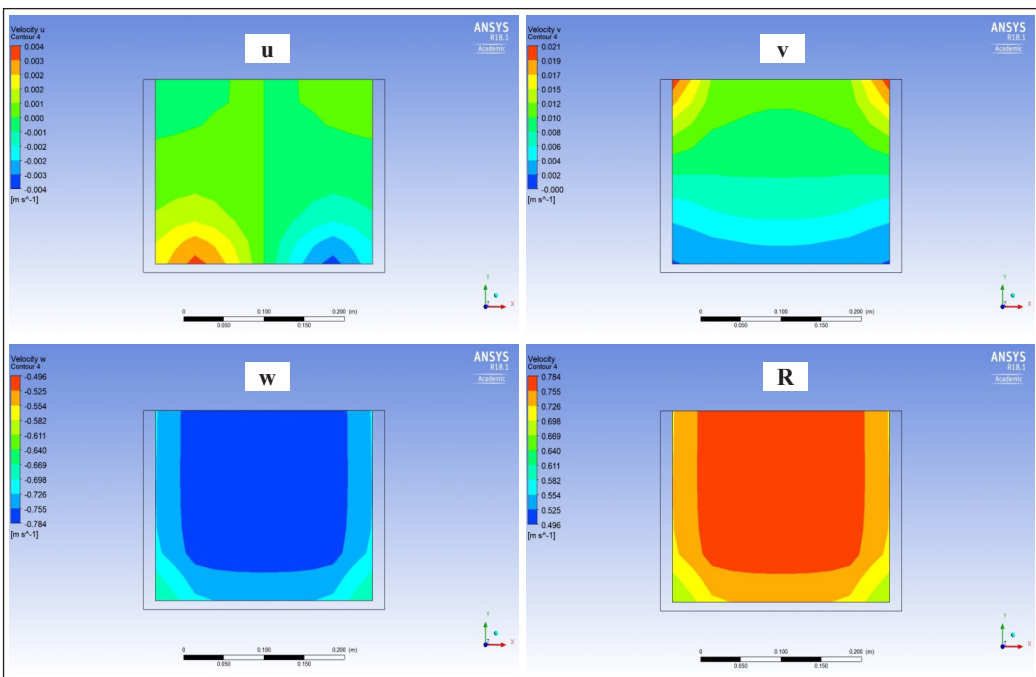
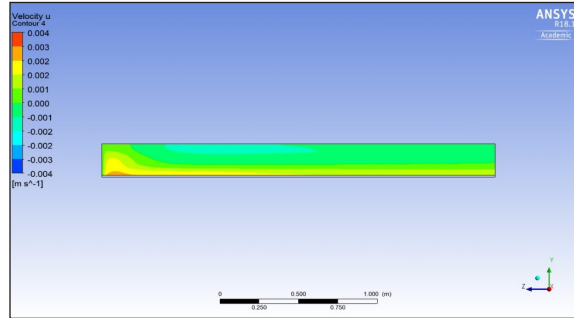
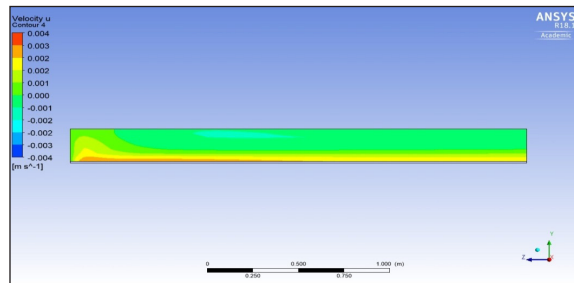


Figure 8. Contours for stream wise (u), velocity vertical velocity (v), lateral velocity (w), resultant velocity (R) at 2.25m from head

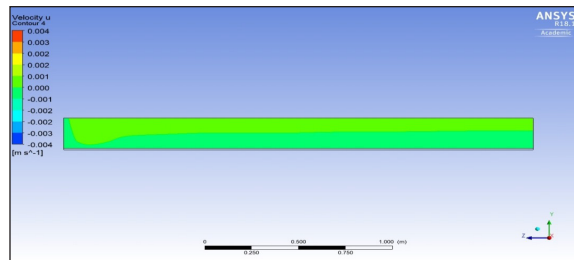
Figure 9 shows the velocity distribution contours across the flow cross-section at 0.03, 0.09, 0.15 m from the side walls simulated in ANSYS in no load condition.



(a)



(b)



(c)

Figure 9. Stream-wise velocity in lateral direction at (a) 0.03m, (b) 0.09m, (c) 0.15m from side wall

RESULTS AND ANALYSIS

Plot of stage vs discharge is represented with the data obtained from the experimental observations performed in the laboratory as shown below in Figure 10. In the Horizontal axis the value represents the discharge in cm^3/sec and the Stage of the flow in m is indicated in vertical axis in m (i.e. the height of flow).

The stream wise, vertical and lateral velocity components obtained from the experimental set up are revealed in Table 2. The results (the resultant velocity) generated from the experimental set up and the numerical analysis is indicated in Table 3. The overall

flow patterns of experimental runs for the rectangular flume are summarized in the graphs. In this paper the results for the test 5 i.e. at depth 0.22 m is shown. In similar way the results of all the other different depths were found out and put for validation.

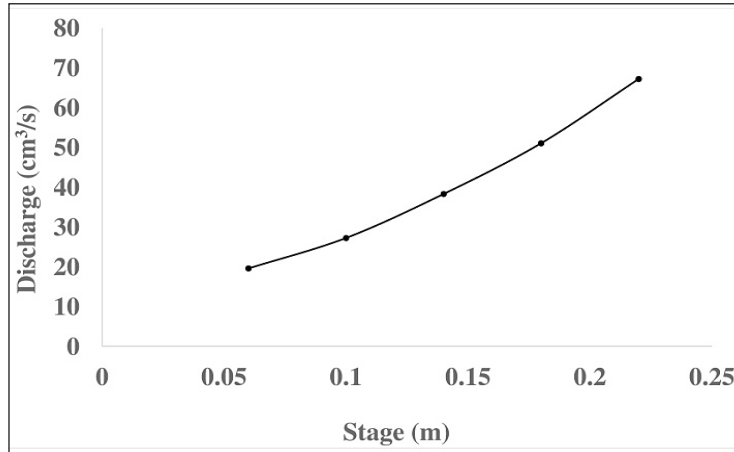


Figure 10. Plot of stage vs discharge

Table 2

Variation of stream wise velocity V_u , vertical velocity V_v , lateral velocity V_w

Height	Stream wise velocity		Vertical velocity	Lateral velocity
	Numerical	Experimental	Numerical	Numerical
0.01	0.000915	0.00086	-0.00021	-0.50673
0.03625	0.001122	0.001043	-0.0003	-0.5469
0.0625	0.001305	0.001226	-0.00036	-0.60262
0.115	0.001405	0.001321	-0.0004	-0.63509
0.14125	0.00148	0.001391	0.000105	-0.67234
0.1675	0.001553	0.001459	0.00016	-0.72495
0.19375	0.001494	0.001394	0.000252	-0.72651
0.22	0.001391	0.001294	0.00028	-0.72718

Table 3

Variation of resultant velocity (V_r)

Height	Numerical	Height	Numerical
0.005	0.1	0.05	0.585
0.015	0.2	0.0625	0.602618
0.022	0.281	0.08875	0.624936
0.027	0.37	0.115	0.666846
0.03	0.41	0.14125	0.711448
0.033	0.46	0.1675	0.730029
0.035	0.523	0.19375	0.712568
0.039	0.558	0.22	0.696472
0.044	0.57		

Graphs were plotted using the data extracted from ANSYS by placing plates at different intervals for purpose of velocity profile analysis. The numerical data obtained were compared to experimental data. Figure 11 shows the comparison of stream-wise velocity profile between experimental and numerical results. From the present study, it can be seen that magnitude of velocity is maximum at some point below free surface as in case of narrow channels which is true for both the experimental and numerical simulation. Variations of vertical velocity profile obtained from the numerical simulation are shown in Figure 12. It is seen that magnitude of velocity gives negative values to nearly mid height with respect to depth of flow and then changes to positive values of velocity (Song and Cox, 1993; Pittaluga & Imran, 2014). Figure 13 represents the variation of velocity in lateral direction. The flow characteristics give all negative magnitude of velocity.

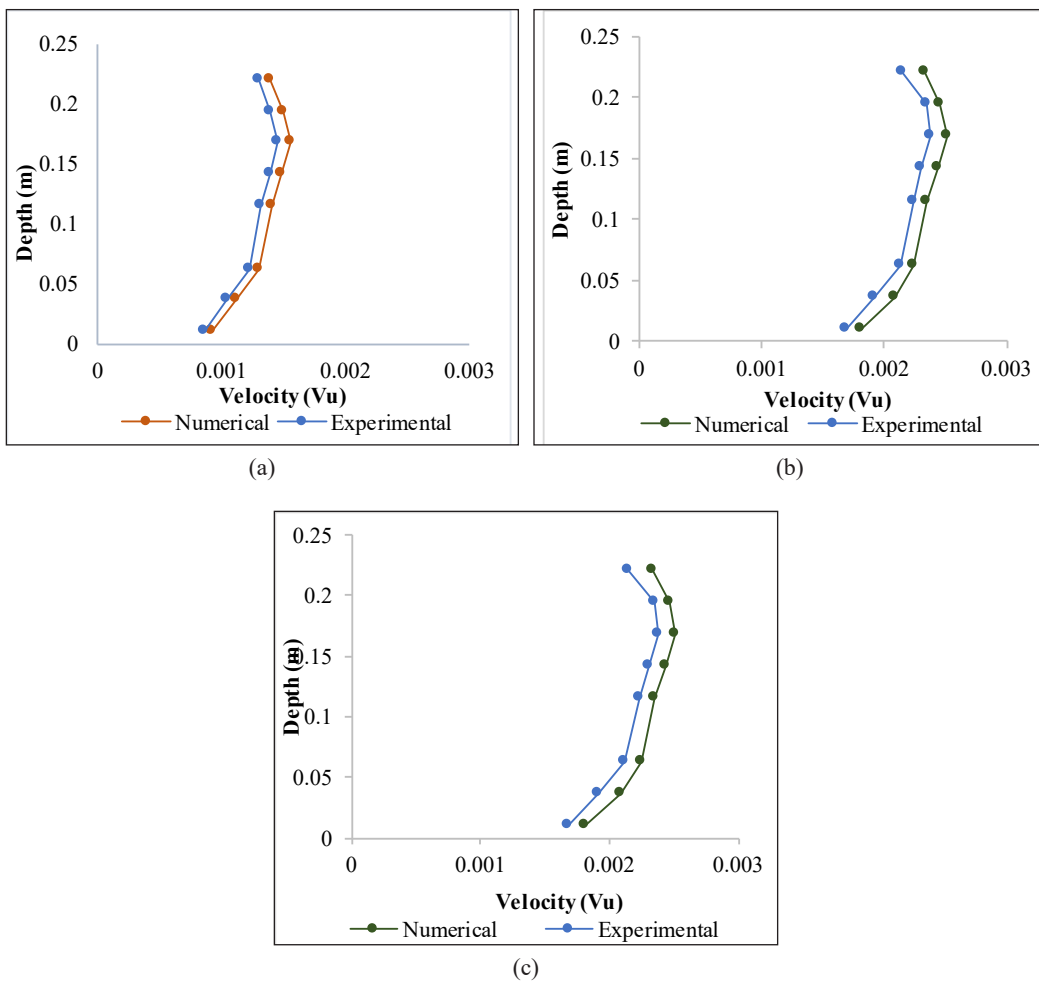
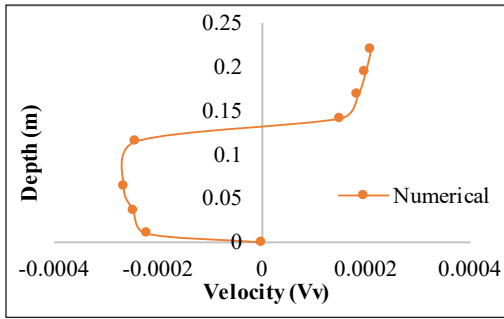
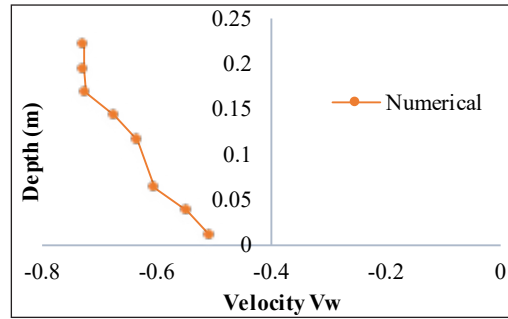


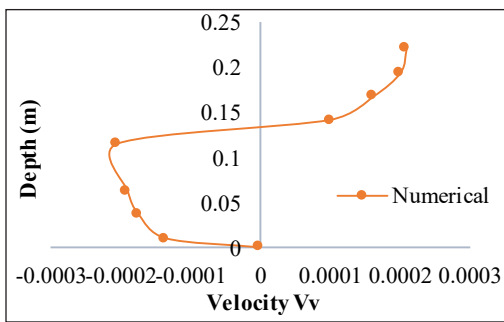
Figure 11. Variation of stream wise velocity comparison for numerical and experimental result at (a) 0.25 m, (b) 1.5m, (c) 2.25m from head gate



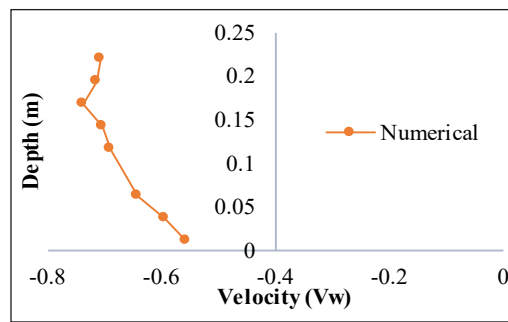
(a)



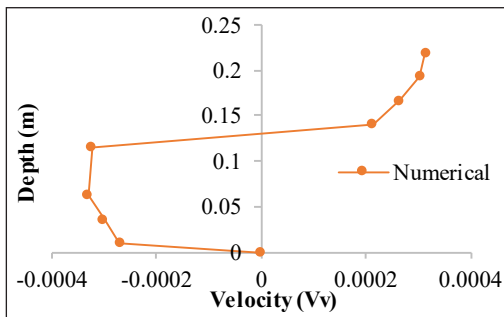
(a)



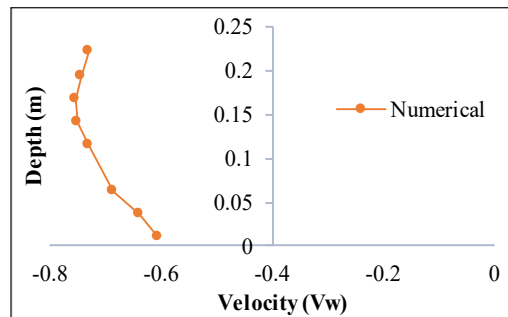
(b)



(b)



(c)



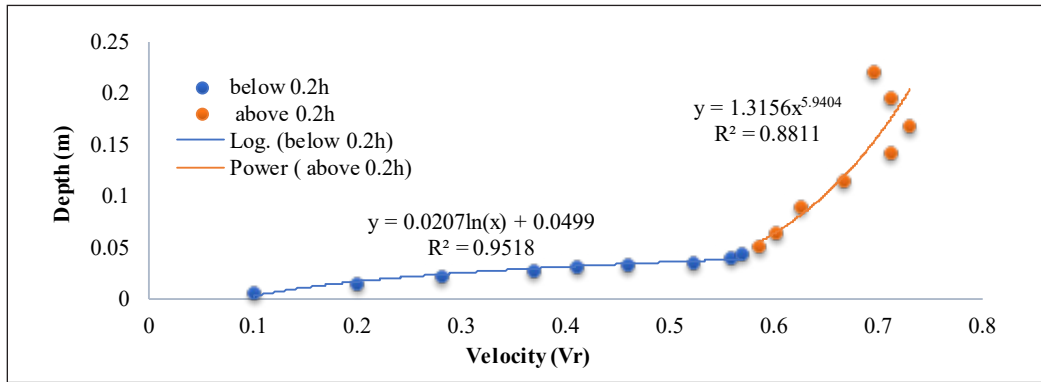
(c)

Figure 12. Variation of vertical velocity for numerical result at (a) 0.25 m, (b) 1.5m, (c) 2.25m from head gate

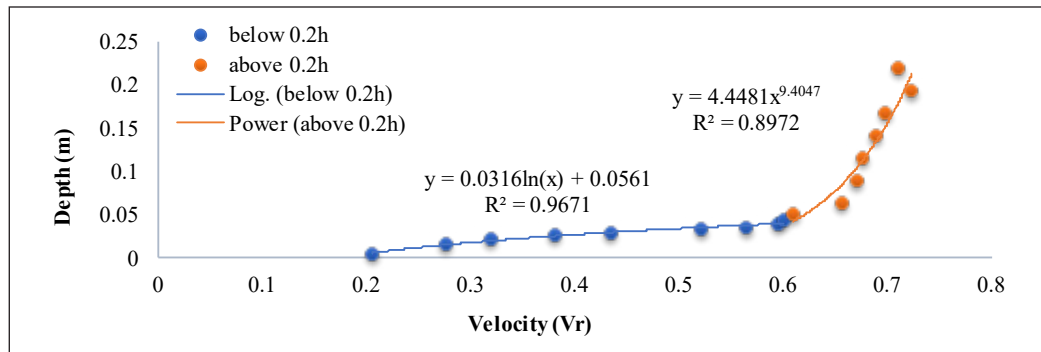
Figure 13. Variation of Lateral velocity for numerical result at (a) 0.25 m, (b) 1.5m, (c) 2.25m from head gate

The variation of resultant velocity profile found out by numerical simulation concerning universal laws (Log and Power Law) is shown in Figure 14. It is observed that the characteristics of flow profile below $0.2h$ (h -depth of flow) obeys Log law and above $0.2h$ follows the Power law (Sarma et al., 1983; Castro-orgaz & Dey, 2011). The R^2 values from the resulting trend line show that the magnitude of velocity obtained best fit to the universal laws. The equation of the two lines is given by 'y' which can be clearly indicated

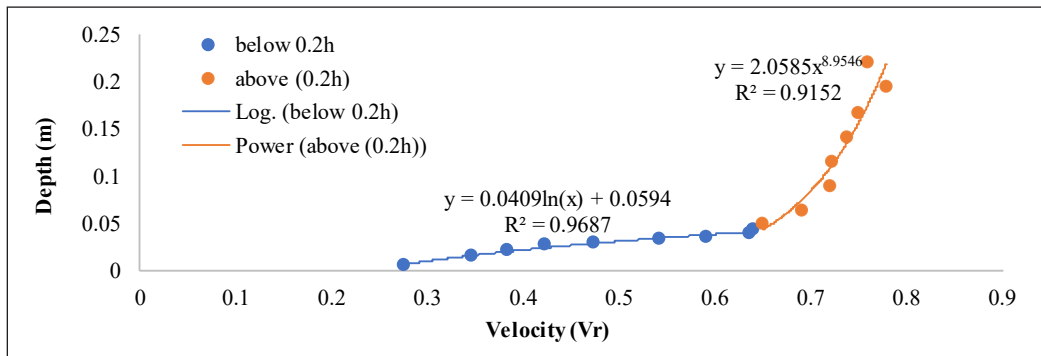
as the inner region follows a logarithmic path and the outer region follows an exponential path. Figure 15 represents the comparison of stream-wise velocity between experimental and numerical results at 0.03, 0.09 and 0.15m from side wall across the flow cross-section.



(a)

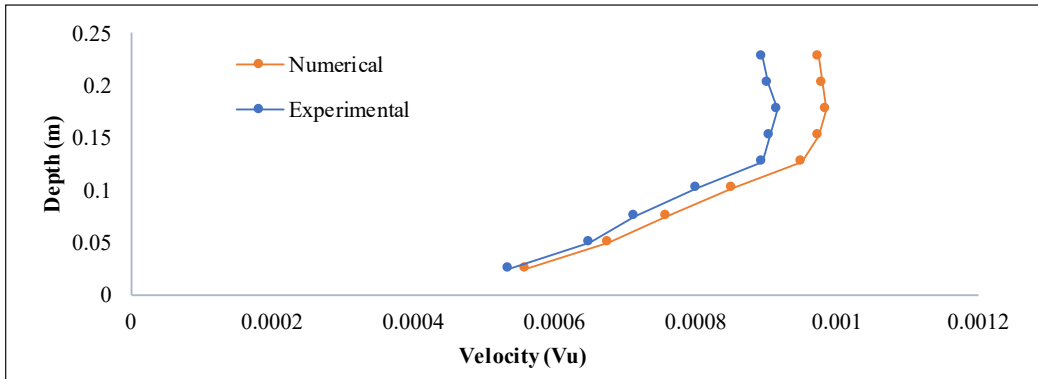


(b)

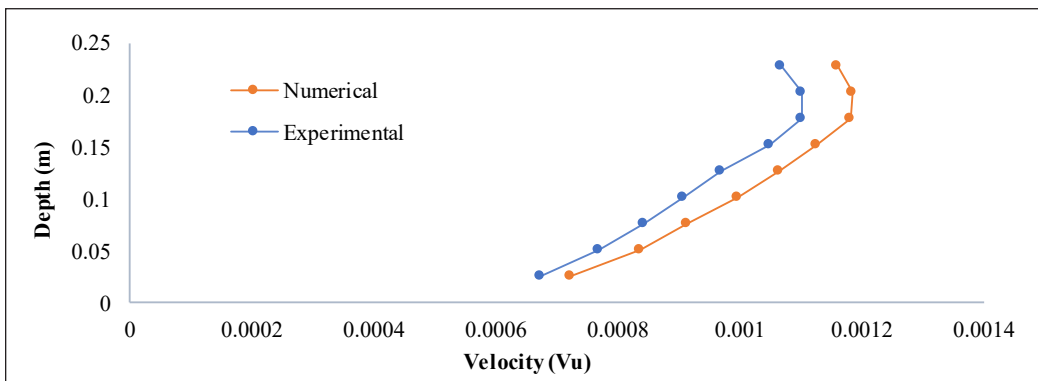


(c)

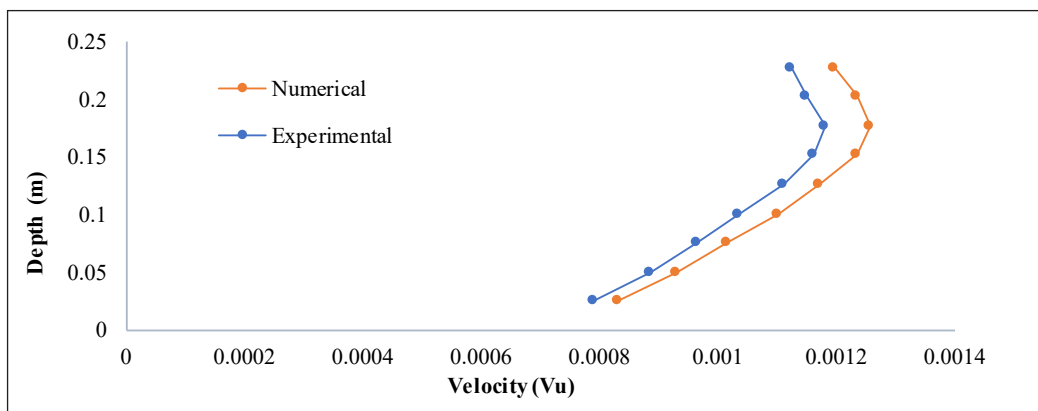
Figure 14. Resultant velocity concerning to Log Law and Power Law at (a) 0.25m, (b) 1.25m, (c) 2.25m from head gate



(a)



(b)



(c)

Figure 15. Stream wise velocity comparison for numerical and experimental result at (a) 0.03m, (b) 0.09m, (c) 0.15m from side wall

Analysis

The velocity profile can be broken into two regions such as the inner region, below $0.2h$ and the outer region, above $0.2h$ (where h =depth of flow). Velocity profile can be demonstrated by the law of logarithmic distribution and with the help of a power law distribution up to the point of maximum velocity. As per universal velocity profile laws, the region below $0.2h$ always follows logarithmic law and the region above $0.2h$ follows power law. The experimental data and the numerical data extracted show that the velocity profile drawn here fits well with the universal velocity profile laws.

CONCLUSION

In present scenario, the experimental and numerical investigation for prediction of velocity for *flow* over plain bed is shown. In the *primary* stage of the present study, a 3D turbulence model for flow over plain bed was simulated utilising $k-\epsilon$ closure model. With the help experimental and numerical results, deviation in values for velocity of *flow* was presented using contour mapping. The main distinguishing point between the velocity distribution in laminar and turbulent flow conditions is that in case of flow to be laminar, the peak velocity occurs at top surface of water while for most turbulent flow situations, the peak velocity is found to be at some point below the water surface which is in case of an open channel cross-section.

- It is examined that the peak velocity is not found at the water surface; rather it occurs at some point below the top surface of water because of effect of turbulence in the rectangular flume used for experiment during the fluid flow (Cardoso et al., 1989).
- The velocity dip is visible from the experimental results but in ANSYS inadequacy of numerical modelling is observed which is often reasonable as the source of computation are not worth to produce such *better* results.
- Additionally, at point when there is effect of sidewall, a lateral velocity component (w) is harmonized close from sidewall of the channel to centre of channel and a down *flow* (v) occurs from top water surface. The components of secondary *flow* give the magnitude of maximum velocity below the top water surface. This is observed for high depth of *flow*.
- Inner region of the flow depth is considered from bed of the channel to 0.2 of the height of flow which follows the Logarithmic law, whereas from above 0.2 of the flow height up to the top water surface is the outer region which follows the power law.
- From the Figure 9 it can be found out that the numerical results are showing error within 10% with respect to the experimental results. The best results are obtained

for highest flow depth. For lowest flow depth, maximum deviation is observed because of effect of boundary layer on the flow parameters.

- As it is observed from Figure 13, variation of velocity in vertical and lateral direction, the numerical results could only be found out using ANSYS, because of the use of Pitot tube which is usually a 1-D instrument and only measures the stream-wise velocity.

ACKNOWLEDGEMENT

We thank the anonymous reviewers and editors for their useful suggestion to develop this manuscript.

REFERENCE

- Absi, R. (2011). An ordinary differential equation for velocity distribution and dip-phenomenon in open channel flows. *Journal of Hydraulic Research*, 49(1), 82-89.
- Afzal, N., Seena, A., & Bushra, A. (2007). Power law velocity profile in fully developed turbulent pipe and channel flows. *Journal of Hydraulic Engineering*, 133(9), 1080-1086.
- Bonakdari, H., Baghalian, S., Nazari, F., & Fazli, M. (2014). Numerical analysis and prediction of the velocity field in curved open channel using artificial neural network and genetic algorithm. *Journal of Engineering Applications of Computational Fluid Mechanics*, 5(3), 384-396.
- Cardoso, A. H., Graf, W. H., & Gust, G. (1989). Uniform flow in a smooth open channel. *Journal of Hydraulic Research*, 27(5), 603-616.
- Castro-Orgaz, O., & Dey, S. (2011). Power-law velocity profile in turbulent boundary layers: An integral Reynolds-number dependent solution. *Acta Geophysica*, 59(5), 993-1012.
- Coles, D. (1956). The law of the wake in the turbulent boundary layer. *Journal of Fluid Mechanics*, 1(2), 191-226.
- Guo, J., & Julien, P. Y. (2006, May 21-25). Application of modified log-wake law in open-channels. In *World Environmental and Water Resource Congress 2006: Examining the Confluence of Environmental and Water Concerns* (pp. 1-9). Omaha, Nebraska, United States.
- Issa, R. I. (1986). Solution of the implicitly discretised fluid flow equations by operator-splitting. *Journal of Computational Physics*, 62(1), 40-65.
- Kang, H., & Choi, S. U. (2006). Reynolds stress modelling of rectangular open-channel flow. *International Journal for Numerical Methods in Fluids*, 51(11), 1319-1334.
- Larocque, L. A., Imran, J., & Chaudhry, M. H., (2013). 3D numerical simulation of partial breach dam break flow using the LES and k- ϵ turbulence models. *Journal of Hydraulic Research*, 51(2), 145-157.
- Naik, B., Khatua, K. K., Wright, N., Sleight, A., & Singh, P. (2018). Numerical modeling of converging compound channel flow. *ISH Journal of Hydraulic Engineering*, 24(3), 285-297.
- Naot, D., Nezu, I., & Nakagawa, H. (1993). Hydrodynamic Behaviour of Compound Rectangular Open

- Channels. *ASCE Journal of Hydraulic Engineering*, 119(3), 390-408.
- Nezu, I., & Rodi, W. (1986). Open-channel flow measurements with a laser Doppler anemometer. *Journal of Hydraulic Engineering*, 112(5), 335-355.
- Pittaluga, M. B., & Imran, J. (2014). A simple model for vertical profiles of velocity and suspended sediment concentration in straight and curved submarine channels. *Journal of Geophysical Research: Earth Surface*, 119(3), 483-503.
- Sarma, K. V. N., Lakshminarayana, P., & Rao, N. S. L. (1983). Velocity distribution in smooth rectangular open channels. *Journal of Hydraulics Engineering*, 109(2), 270-289.
- Sarma, N. V. K., Prasad, R. V. B., & Sarma, K. A. (2000). Detailed study of binary law for open channel. *Journal of Hydraulics Engineering*, 126(3), 210-214.
- Song, R., & Cox, S. K. (1993, June 14-17). Vertical velocity in cirrus case obtained from wind profiler. In *Proceedings of a Conference on the FIRE Cirrus Science* (pp. 153-156). Breckenridge, Colorado, United States.
- Welahettige, P., Lie, B., & Vaagsaether, K. (2017). Flow regime changes at hydraulic jumps in an open Venturi channel for Newtonian fluid. *The Journal of Computational Multiphase Flows*, 9(4), 169-179.
- Wilkerson, V. G., & McGahan, J. L. (2005). Depth averaged velocity distribution in straight trapezoidal channel. *Journal of Hydraulics Engineering*, 131(6), 509-512.